



# Detection of high and moderate crustal strain zones in Uttarakhand Himalaya, India

Rakesh K. Dumka<sup>1</sup> · Bahadur Singh Kotlia<sup>2</sup> · Girish Ch. Kothiyari<sup>1</sup> · Joydeep Paikrey<sup>1</sup> · Siddharth Dimri<sup>1</sup>

Received: 14 September 2017 / Accepted: 14 July 2018 / Published online: 23 July 2018  
© Akadémiai Kiadó 2018

## Abstract

We present geodetically estimated crustal strain rates in Uttarakhand Himalaya, a region which has long been considered as a part of seismic gap. We processed and analyzed the GPS data, acquired from the sites enveloping all the litho-tectonic units from the Sub Himalaya in the south to the Tethys Himalaya in the north together with the major Himalayan thrust/fault systems. On the basis of the obtained dataset, we conclude that the maximum amount of crustal shortening takes place towards the hinterland in the vicinity of Main Central Thrust and Inner Lesser Himalaya which is also in agreement with high seismic activity in these sectors. The GPS velocities of the sites (Indian reference frame) show significant variation from the sub-Himalaya to the Tethys Himalaya. The Sub and Inner Lesser Himalayan parts exhibit low deformation rate in contrast to the maximum amount of deformation in the Inner Lesser and Higher Himalayan segments. The strain analysis reveals lateral variation with high strain zones (HSZ) and moderate strain zones (MSZ) within the compressional regime in the Uttarakhand Himalaya. The strain rate of 0.45 and 0.25 micro-strain/year is observed in the HSZ and MSZ respectively. By comparing the strain rate with the seismicity pattern for the past five decades, we suggest that the earthquakes in the HSZ are related with ramp structure of the MHT, whereas, part of accumulated strain in the MSZ is being released in form of the present day seismic activity.

**Keywords** Crustal strain · GPS geodesy · GAMIT-GLOBK software · Uttarakhand Himalaya

---

**Electronic supplementary material** The online version of this article (<https://doi.org/10.1007/s40328-018-0226-z>) contains supplementary material, which is available to authorized users.

---

✉ Rakesh K. Dumka  
rkdumka@gmail.com

<sup>1</sup> Institute of Seismological Research, Raisan, Gandhinagar 382009, India

<sup>2</sup> Centre of Advanced Study in Geology, Kumaun University, Nainital 263002, India

## 1 Introduction

GPS based geodetic studies suggest variation in the rate of convergence and deformation of the Indian plate along the Himalaya, across which about 50% of India–Eurasia convergence has been estimated to take place (Avouac and Tapponier 1993). The GPS results in the Kashmir Himalaya indicate arc-normal convergence of about 14 mm/year (Jade et al. 2014) and 5 mm/year of dextral motion on the Karakorum Fault system (Kundu et al. 2014). The convergence rate in the Garhwal Himalaya region has been estimated at about 14 mm/year (Banerjee and Bürgmann 2002; Jade 2004). Similarly, a convergence rate of 10–15 mm/year in the Kumaun Himalaya province has been approximated (Jade et al. 2014; Dumka et al. 2014a, b). The GPS derived convergence rate in the Nepal Himalaya has been calculated at about 18–20 mm/year (Bilham et al. 1997; Jouanne et al. 1999; Ader et al. 2012). Furthermore, this rate varies between 15 and 21 mm/year in the northeast Himalaya (Jade et al. 2007, 2017; Banerjee et al. 2008; Mukul et al. 2010; Stevens and Avouac 2015) (see Fig. 1). Based on the GPS derived slip and strain rate estimations, Bilham et al. (1997, 1998, 2001) proposed possibility of a great earthquake in the eastern Nepal Himalaya. Throughout the Himalaya, most of the crustal deformation is localized on the Main Himalayan Thrust (MHT) and its surface trace is known as the Himalayan Frontal Thrust (HFT) (Nakata 1989; Hauck et al. 1998; Cattin and Avouac 2000; Lavé and Avouac 2000; Ader et al. 2012). Based on the arc-parallel gravity anomaly analysis, Hetényi et al. (2016) have suggested disparate flexural geometry in the four segments of the Himalaya. According to Stevens and Avouac (2015), about 100 km width of the MHT is entirely locked along the Himalayan arc. On the whole, the MHT is locked to a depth of about 20 km from the surface over a width of about 115 km towards the western part of Nepal (Bettinelli et al. 2006; Zhao and Nelson 1993; Nelson 1996; Cattin and Avouac 2000) and the down-dip creeping rate is comparable with the geological slip rate (Pandey et al. 1995; Bilham et al. 1997; Larson et al. 1999; Jouanne et al. 1999, 2004).

Due to the intense stress accumulation at the down-dip edge of the MHT, a substantial seismic activity has been observed along the front of the higher Himalaya (Pandey et al. 1999; Cattin and Avouac 2000; Arora et al. 2012). According to Ader et al. (2012), the width of the locked zone is estimated at 80–100 km in the central Nepal Himalaya, and that an earthquake of  $M_w \sim 8$  is required to balance the measured slip deficit. Mugnier et al. (2013) suggested that a great earthquake could occur anytime at all along the front of the central Himalaya. After the 2015 Nepal earthquake, Avouac et al. (2015) showed that the west of this earthquake, the area between the 2015 rupture and the 1905 Kangra ( $M_w 7.8$ ) event has been locked for over 500 years with a slip deficit of 10 m. Based on the receiver function study in the Uttarakhand Himalaya, Caldwell et al. (2013) indicated presence of ramp beneath the trace of the Munsiary Thrust. The trench investigations along the HFT in Kumaun Himalaya also reveal seismic inactivity during the last 700 years, giving indication to a great earthquake in this region (Rajendran et al. 2015). The tectonic activities are more common towards the zone of HFT-foreland side (Nakata 1982, 1989; Le Fort 1975; Valdiya 2003; Thakur 2004).

In Uttarakhand, the rate of convergence varies between 14 and 12 mm/year in the Garhwal and Kumaun Himalaya respectively (Jade 2004, 2014). The horizontal shortening of  $< 7$  mm/year between IISC (Peninsular India) and GBPK (Lesser Kumaun Himalaya) reveals that the frontal part of the Himalaya is presently locked with the Indian Plate and that the Higher Himalaya is converging towards the Lesser Himalaya at a rate of about 9–16 mm/year (Dumka et al. 2014a, b). The campaign mode study in the Lesser Kumaun Himalaya (Ponraj

et al. 2010, 2011) also indicates the accommodation of the maximum crustal strain near the Main Central Thrust (MCT).

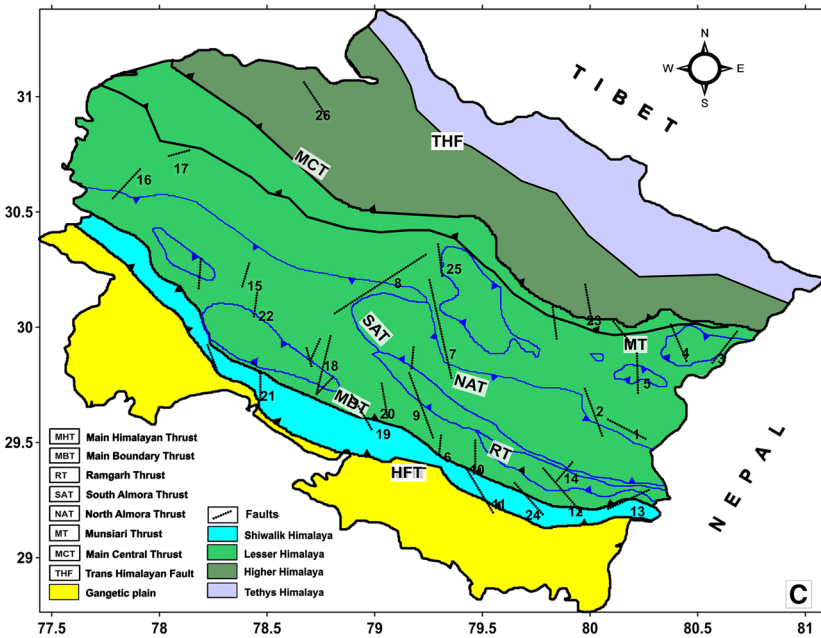
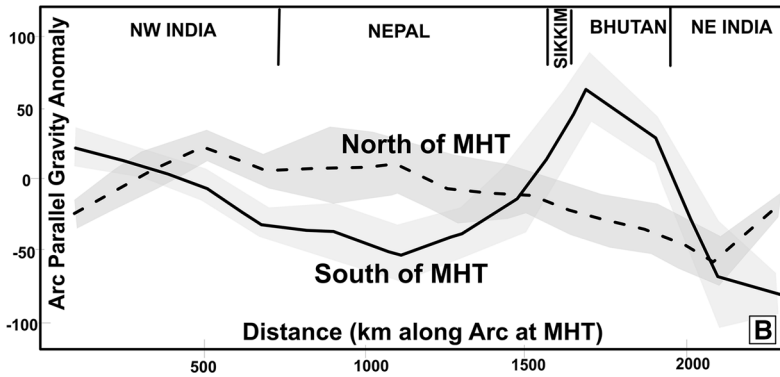
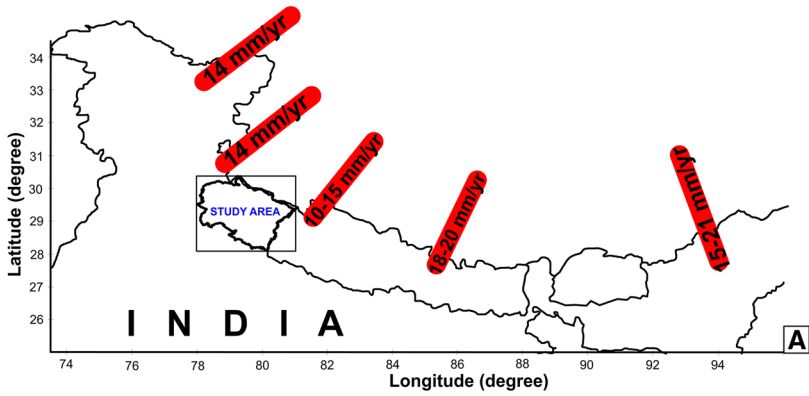
Our current study attempts to understand the deformation and strain pattern in the Uttarakhand state as a whole (Fig. 1) by analyzing the GPS results of 15 new campaign mode sites in addition to published datasets (e.g., Banerjee and Bürgmann 2002; Ponraj et al. 2010, 2011; Jade et al. 2014; Dumka 2011; Dumka et al. 2014a, b). Based on the combined data, we recognized the zones of maximum crustal deformation and strain. The active nature of faults and uplift rate of river terraces in the study area are linked with the higher deformation rates. Finally, the achieved information is correlated with the earthquake distribution of the region and this may be useful for future hazard management of this hill state.

## 2 Tectonic setting

Tectonically one of the most active Himalayan segments, the Uttarakhand Himalaya constitutes four litho-tectonic units from south to north; Sub-Himalaya, Lesser Himalaya, Higher Himalaya and Tethys Himalaya, which are delimited by the Himalayan Frontal Thrust (HFT), Main Boundary Thrust (MBT), Main Central Thrust (MCT) and Trans Himadri Fault/South Tibetan Detachment Fault (THF/STDF), respectively (see Fig. 1). Besides these intracrustal boundary thrusts, a number of local thrust systems lie in between, the major ones being the Ramgarh Thrust (RT), South Almora Thrust (SAT), North Almora Thrust (NAT) and Munsari Thrust (MT) from south to north (Gansser 1964; Jhingran et al. 1976; Valdiya 1979, 1999; Nakata 1989; Thakur 1992; Godin 2003). Also, the faults/thrusts, oblique or parallel to the main intracrustal boundary thrusts, are predominantly oriented NW/NNW-SE/SSE (Middlemiss 1890a, b; Gansser 1964; Valdiya 1976; Valdiya and Kotlia 2001) and many of these were formed during the Quaternary period (i.e., Kotli Fault, Bhimtal-Naukuchiatal Fault, Banlekh Fault, Ladhiya Fault, Bisoriya Fault, Bhikiyasain Fault, Dulam Fault, Garampani Fault, Betalghat–Basgaon Fault, Kosi Fault, Alaknanda Fault, Chaukhotia Fault, Nandprayag Fault (See Fig. S1) (Valdiya 1976, 1993, 2003; Nakata 1982; Kotlia et al. 1997, 2000, 2008, 2010; Valdiya and Kotlia 2001; Kotlia and Rawat 2004; Thakur 2004; Rawat and Kotlia 2006; Sati et al. 2007; Mehta and Sanwal 2011; Kotlia and Joshi 2013; Rana et al. 2013; Joshi and Kotlia 2014) and these are considered to be active and thus responsible for damming the ancient rivers/streams, resulting in formation of palaeolakes (Kotlia et al. 1997, 2008, 2010; Valdiya and Kotlia 2001). The studies on the uplift due to such active faults/thrusts can be well corroborated with the seismic activity (e.g., Arora and Mahashabde 1987; Shrikande et al. 2006; Lyubushin et al. 2010; Roy and Mondal 2012).

## 3 Methodology and data

The GPS data from 15 campaign mode stations together with previously published results from 43 sites (e.g., Banerjee and Bürgmann 2002; Ponraj et al. 2010, 2011; Jade et al. 2014; Dumka et al. 2014a, b) (see Table 1) were analyzed. The raw GPS data from 15 sites were converted into the RINEX (Receiver Independent Exchange) format using the TEQC program (translation, editing and quality control), distributed by UNAVCO (University NAVSTAR Consortium) (Estey and Meertens 1999). This program provides a synopsis containing L1/L2 tracking status for each SV session's start



◀ **Fig. 1** **a** Convergence rate of various segments throughout the Himalaya (based on Banerjee and Bürgmann 2002; Jade 2004; Jade et al. 2007, 2014; Banerjee et al. 2008; Mukul et al. 2010; Ader et al. 2012; Dumka et al. 2014a, b; Stevens and Avouac 2015). **b** Shows the arc parallel gravity anomaly along the Himalaya (Hetényi et al. 2016). Four litho-tectonic units in Uttarakhand Himalaya (Sub-Himalaya, Lesser Himalaya, Higher Himalaya and Tethys Himalaya), demarcated by major thrust/fault systems. Dotted lines show subsidiary thrusts/faults. Details of subsidiary faults with geology are given in Fig. S1

and end time, data logging interval, list of satellite observed and missing observations, clock drift rate/gaps, number of cycle slips and session length. These parameters are most important factors for quality inspection of the GPS data and are useful for data processing. To improve the uncertainties in relative positioning measurements, both L1 and L2 frequencies of several satellites must be present in the data (Blewitt 1989; Dong and Bock 1989). The multipath report is important parameter for assessment of the site-specific errors while the session length of data is important for reduction in the RMS values (Snay et al. 2002; Satirapod et al. 2001). The dataset was post-processed using GAMIT-GLOBK-GLORG software, developed by MIT, USA (King and Bock 1998; Herring et al. 2010) to obtain constrained solution (H-) files of parameter estimates and covariance (Herring et al. 2006). We selected a set of sites with applied constraint to minimize the adjustment of the network (Herring et al. 2006).

In GAMIT, Zenith tropospheric delay for each station was estimated by a linear model with stochastic constraint for signal delay due to the troposphere. The basic input for the GAMIT are the observation files of permanent/IGS stations in the RINEX format, orbital file (sp3 files) or g-files and the global navigation files. The orbital and IGS-RINEX files are available at Scripps Orbit and Permanent Array Centre (SOPAC) and brdc files are assessable at Continuously Operating Reference Stations. After combining the daily solutions, velocities of all the stations were estimated in the ITRF08 reference frame. To account for temporal correlation in the time series, we used random walk noise at the level of  $0.75 \text{ mm year}^{-1/2}$  (Mao et al. 1999). For improved understanding of the deformation pattern, velocities of all the sites were calculated in the Indian Reference Frame (Mahesh et al. 2012) (see Fig. 2). However, to avoid any discrepancy due to combining results of different reference frames, velrot tool of the GLOBK (Herring et al. 2010) was used for conversion and all the velocities were estimated in the ITRF08 reference frame. For calculation of deformation rate at each site, Euler pole of the Indian plate (e.g., Ader et al. 2012; Mahesh et al. 2012; Jade et al. 2014) was used.

The strain fields of the area were calculated following a method proposed by Pesci and Teza (2007) and Teza et al. (2008). This method provides a clear-cut calculation of major and minor strain axes. The strain field was computed on the nodes of  $8 \times 8 \text{ km}$  grid via Least Square (LS) method which is based on rescaling of the covariance matrix of velocity data by weighting function which takes into account the distances between the grid node and the GPS stations (e.g., Shen et al. 1996; Pesci et al. 2009). Errors are rescaled by means of weight function,  $\exp(-\delta d/d_0)$  (Pesci and Teza 2007), where  $d$  is distance between the knot and  $d_0$  is smoothing constraint (Shen et al. 1996; Pesci and Teza 2007; Pesci et al. 2009). Smoothing constraint was considered as three times the grid spacing (Livieratos 1980; Shen and Jackson 2000). If the data points are widely distributed, the local strain can be estimated at each knot of the grid (or in a defined point) using weighting strategy (see Shen and Jackson 2000; Pesci and Teza 2007; Pesci et al. 2009).

A significance test was conducted for various grid intervals, i.e., 5, 8, 12, 15, 20, 25 km and finally we chose 8 km grid interval as it is significant for strain analysis of study area (Fig. S2). The significance test detects the points which can be considered as actual

**Table 1** Velocities of all the GPS sites with respect to the Indian plate (Mahesh et al. 2012) and tectonic position of the GPS sites

Site	Lat	Long	$V_e$ (mm/year)	$\sigma V_e$ (mm/year)	$V_n$ (mm/year)	$\sigma V_n$ (mm/year)	Reference and data availability	Tectonic segment
MLRI	30.70	79.90	-6.70	0.90	-4.80	1.00	Jade et al. (2014)	Tethys
TOPI	30.50	80.20	-6.80	1.10	-5.50	1.40	Present study (2014–2016)	Tethys
BELJ	30.40	80.20	-5.80	1.30	-6.40	1.50	Present study (2014–2016)	Tethys
BRFU	30.40	80.20	-5.00	0.80	-6.60	0.90	Dumka et al. (2014a)	Tethys
MILA	30.40	80.20	-7.60	0.90	-5.50	1.00	Dumka et al. (2014a)	Tethys
MART	30.30	80.20	-6.50	1.20	-4.80	1.30	Dumka et al. (2014a)	Tethys
GUNJ	30.20	80.90	-6.10	1.30	-4.60	1.40	Dumka et al. (2014a)	Tethys
KALA	30.20	80.90	-5.50	1.10	-3.70	1.20	Dumka et al. (2014a)	Tethys
NABH	30.20	81.00	-6.80	0.41	-4.40	1.20	Dumka et al. (2014a)	Tethys
GARB	30.10	80.90	-6.40	0.51	-6.10	1.40	Dumka et al. (2014a)	Tethys
RBAG	29.64	79.43	0.27	0.77	0.83	0.93	Present study (2004, 2005, 2014–2016)	Sub
RAMR	29.23	79.08	-2.48	0.34	0.67	0.74	Ponraj et al. (2011)	Sub
HALD	29.21	79.51	0.52	0.35	0.67	0.78	Ponraj et al. (2011)	Sub
PILJ	28.63	79.85	-1.15	0.59	0.71	0.82	Ponraj et al. (2011)	Sub
SUKI	31.00	78.70	-8.90	0.70	-4.90	1.00	Present study (2014–2016)	MCT
OKHI	30.52	79.09	-4.80	1.10	0.73	0.83	Jade et al. (2014)	MCT
TUGN	30.50	79.20	-5.30	0.70	-8.10	0.90	Jade et al. (2014)	MCT
KHLL	30.29	79.21	-1.20	0.35	0.71	0.79	Jade et al. (2014)	MCT
LILM	30.20	80.20	-7.90	1.10	-7.70	1.30	Dumka et al. (2014a)	MCT
CHIR	30.10	80.60	-8.70	1.10	-4.40	1.20	Present study (2014–2016)	MCT
KHAL	30.10	80.20	-7.20	0.80	-4.40	0.90	Jade et al. (2014)	MCT
MUNS	30.10	80.20	-8.90	1.10	-4.20	1.30	Dumka et al. (2014b)	MCT
MUNT	30.10	80.20	-9.30	0.80	-4.90	0.90	Jade et al. (2014)	MCT
MUNV	30.10	80.20	-9.80	0.80	-4.40	0.90	Jade et al. (2014)	MCT
MUNS	30.06	80.20	6.98	1.15	0.64	0.73	Ponraj et al. (2011)	MCT

Table 1 (continued)

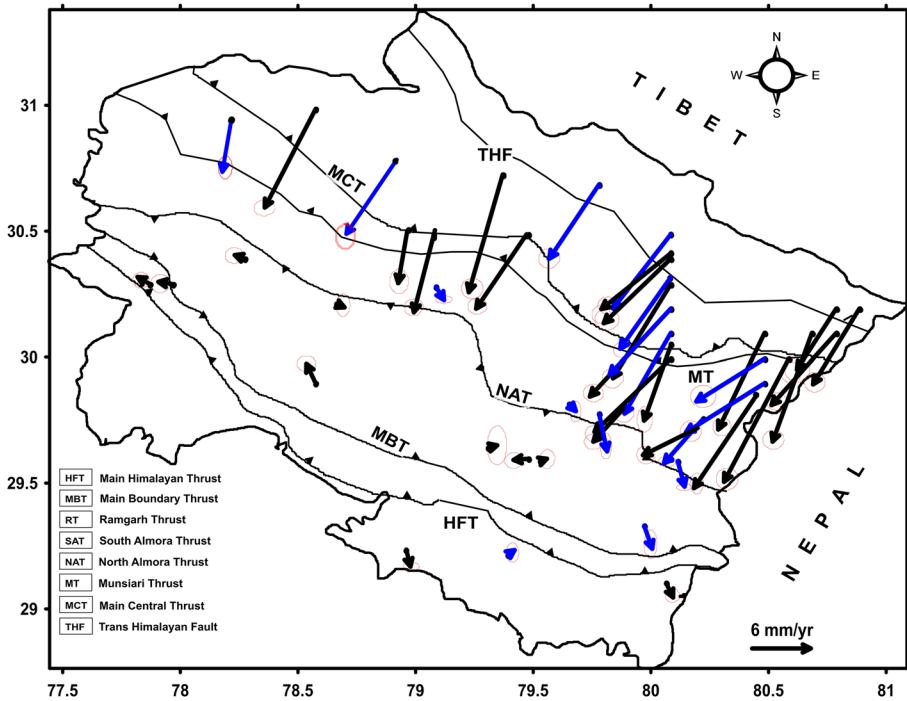
Site	Lat	Long	$V_e$ (mm/year)	$\sigma V_e$ (mm/year)	$V_n$ (mm/year)	$\sigma V_n$ (mm/year)	Reference and data availability	Tectonic segment
GIRG	30.03	80.17	- 11.40	1.60	0.72	0.82	Ponraj et al. (2011)	MCT
BALA	30.00	80.20	- 6.60	1.10	- 7.20	1.30	Dumka et al. (2014a)	MCT
NHPC	29.90	80.60	- 9.70	1.40	- 8.80	1.50	Present study (2004, 2014–2016)	MCT
CHOP	30.49	79.20	1.30	1.30	0.79	0.86	Jade et al. (2014)	Lesser
CHAB	30.40	78.40	0.30	0.70	- 1.00	0.90	Jade et al. (2014)	Lesser
DEHR	30.30	78.10	0.20	1.00	- 1.50	1.10	Jade et al. (2014)	Lesser
WIH2	30.30	78.00	0.60	1.00	- 1.20	1.10	Ponraj et al. (2011)	Lesser
SRIN	30.22	78.79	- 0.36	1.31	0.73	0.83	Ponraj et al. (2011)	Lesser
LANS	29.90	78.70	1.80	0.70	- 0.90	0.90	Jade et al. (2014)	Lesser
DHAR	29.86	80.56	- 10.21	1.20	0.71	0.80	Present study (2004, 2005, 2014–2016)	Lesser
BAGE	29.82	79.77	- 0.65	1.25	0.64	0.73	Present study (2014–2016)	Lesser
BERI	29.80	80.00	- 3.00	0.70	- 2.80	0.90	Present study (2014–2016)	Lesser
KKOT	29.78	79.90	- 3.39	1.64	0.69	0.77	Present study (2014–2016)	Lesser
ASKT	29.76	80.34	- 5.13	0.48	0.74	0.84	Ponraj et al. (2011)	Lesser
BAGO	29.70	80.30	0.10	1.40	- 2.90	1.50	Present study (2014–2016)	Lesser
KANA	29.70	80.30	1.10	1.40	- 7.70	1.50	Dumka et al. (2014b)	Lesser
GBPK	29.60	79.60	- 0.20	0.70	- 1.40	0.90	Dumka et al. (2014a)	Lesser
PGRH	29.60	80.20	0.10	0.70	- 2.30	0.90	Jade et al. (2014)	Lesser
PITH	29.60	80.20	- 0.60	0.70	- 2.00	0.90	Dumka et al. (2014b)	Lesser
ALMO	29.59	79.65	0.17	0.85	0.65	0.72	Ponraj et al. (2011)	Lesser
PITH	29.59	80.23	- 2.39	0.30	0.65	0.74	Ponraj et al. (2011)	Lesser
CHAM	29.33	80.09	- 2.09	1.74	0.73	0.81	Present study (2004, 2005, 2014–2016)	Lesser
BANB	29.10	80.18	- 1.35	0.74	0.69	0.80	Ponraj et al., 2011	Lesser
BDRI	30.74	79.49	- 10.90	1.20	1.92	1.33	Present study (2014–2016)	Higher
AULI	30.50	79.60	0.90	0.70	0.10	0.90	Jade et al. (2014)	Higher

Table 1 (continued)

Site	Lat	Long	$V_e$ (mm/year)	$\sigma V_e$ (mm/year)	$V_n$ (mm/year)	$\sigma V_n$ (mm/year)	Reference and data availability	Tectonic segment
LASP	30.30	80.20	- 8.50	0.90	- 5.50	1.00	Present study (2014–2016)	Higher
BOGD	30.20	80.20	- 5.90	1.20	- 5.80	1.50	Dumka et al. (2014a)	Higher
RGAD	30.20	80.20	- 10.98	1.10	- 5.60	1.30	Present study (2014–2016)	Higher
CHIA	30.10	80.80	- 9.80	1.10	- 3.80	1.30	Dumka et al. (2014b)	Higher
LAMA	30.10	80.80	- 13.50	1.20	- 4.50	1.40	Dumka et al. (2014b)	Higher
JIPT	30.00	80.70	- 11.10	1.20	- 6.10	1.30	Dumka et al. (2014b)	Higher

In the present study, data of minimum 72 h were generated at each site in the mentioned data availability years





**Fig. 2** Velocities of all the sites in the Indian reference frame, showing deformation pattern in the region. Blue arrows indicate velocities of 15 new sites and black arrows the velocities obtained by previous studies (e.g., Ponraj et al. 2010, 2011; Jade et al. 2014; Dumka et al. 2014a, b). (Color figure online)

representative of a local strain at selected scale. The significance test indicates the spatial distribution of the GPS points around grid point at distance lower or equal to the scale factor. If there are three GPS points in  $120^\circ$  area around the grid point at distance lower or equal to the scale factor, then it has high significance. Based on this, we categorized the whole region into three zones, most significant, mid-significant and low-significant (e.g., Pesci and Teza 2007). In the present study, we used the dataset from the most and mid-significant areas only.

## 4 Results

### 4.1 Deformation analysis

Average deformation rate for the Sub Himalayan sites is around  $1.5 \pm 1$  mm/year (with 1 sigma uncertainty) which increases to  $11.3 \pm 1.6$  mm/year for the Higher Himalayan sites. The average deformation rate in the Lesser Himalayan sites is computed at 2.8 mm/year. However, average rate of the GPS sites in the Inner lesser Himalaya is higher ( $5.2 \pm 1.2$  mm/year), compared to that of  $1.7 \pm 1.3$  mm/year in the outer Lesser Himalayan sites (Fig. 3a). The average deformation rate of GPS sites along the MCT zone is observed as  $8.7 \pm 1.7$  mm/year, higher than that of the Lesser Himalaya. This implies that at present

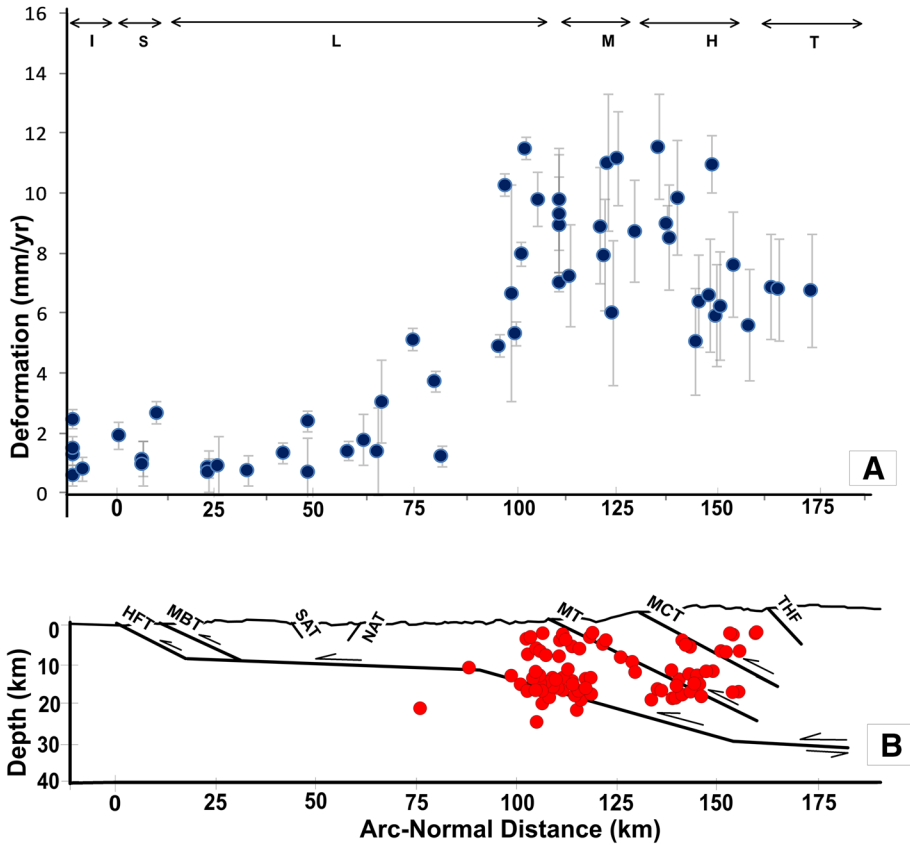


**Fig. 3** **a** Deformation rate from GPS sites (arc-perpendicular distance from the HFT) in different tectonic units of Uttarakhand Himalaya. An abrupt increase in deformation rate is clearly seen in vicinity of the MCT and maximum in the higher Himalaya. The letters in the top of figure are I, Indo-Gangetic plain; S, Sub-Himalaya; L, Lesser Himalaya; M, MCT zone; H, Higher Himalaya; T, Tethys Himalaya. **b** Depth-wise distribution of earthquakes during 2007–2015 in the Kumaun Himalaya (redrawn from Negi et al. 2017) indicating focussed activity near the MHT ramp and thrust faults above. (Color figure online)

most of the Himalayan shortening is mainly concentrated near the NAT, MT and MCT in the Uttarakhand Himalaya. This may suggest that the MHT is locked until the base of the Outer Lesser Himalaya and most of the slip is being accommodated on the root of the hinterland faults.

The seismicity pattern of the region suggests that small and moderate earthquakes occurred on the mid-crustal ramp of the MHT (Seeber and Armbruster 1981; Molnar 1990; Avouac 2003; Gahalaut 2008; Negi et al. 2017) (Fig. 3b). We also conclude that the maximum amount of deformation has occurred in the same vicinity. The distribution pattern of earthquakes (ISC, International Seismological Centre, <http://www.isc.ac.uk>) in the Uttarakhand Himalaya indicates a high concentration in the Higher Himalaya, proving extreme accumulation of the stress at the down-dip edge of the locked MHT.

## 4.2 Strain analysis

The estimated site velocities with respect to the Indian plate were used as an input for the strain analysis. The most crucial finding of the present study is identification of the zones of strain accumulation (Fig. 4a) and these are categorized into High Strain Zones (HSZ) and Moderate Strain Zones (MSZ) based on the magnitude of strain. The zones with strain value greater than 0.3 micro-strain/year are considered as HSZ while less than 0.3 micro-strain/year are considered as MSZ. Accordingly, two (HSZ1, HSZ2) and one (MSZ1) were identified in the study area (Fig. 4a). The distribution pattern indicates lateral variation in the strain value in the study region. Strain rate of 0.4–0.45 micro-strain/year is viewed in the vicinity of the MCT towards the eastern and western part but in the middle part of the study area, the strain rate appears less than 0.2 micro-strain/year. To witness the variation in strain with respect to the MHT, we have drawn three arc normal profiles of strain rate in the region (Fig. 4b). The maximum strain rate of  $\geq 0.45$  micro-strain/year has been detected at a distance of 80 and 110 km from the HFT along Profile I and III, respectively. However, the profile II indicates maximum strain at a distance of 190 km from the HFT. The presence of a ramp is proposed at a distance of 100–130 km north of the MHT (see also Caldwell et al. 2013; Negi et al. 2017). The maximum strain of profile I and III can be associated with the ramp of the MHT but the low strain rate close to the ramp in profile II may be due to other factors, which have to be investigated in the future.

The calculated strain indicates that most of the region is in the compressional regime as expected because of the tectonics of the Indian-Eurasia collision. The maximum compressional strain is calculated in the vicinity of the MT and MCT in both the Garhwal and Kumaun regions (Fig. 5). Variation in the trend of the compression has been observed in the study area, which is perhaps controlled by the strike of the major Himalayan fault systems. The earthquake fault plane solution suggests WNW-ESE to NNW-SSE orientation of the compressional axis (e.g., Stevens and Avouac 2015; Mahesh et al. 2015; Negi et al. 2017). The world stress map (Heidbach et al. 2016) for the study area supports the orientation of the principle axis of deformation (Fig. S3). The orientation of extensional strain tensor is E-W to WNW-ESE which we believe is due to the lateral expansion along the major hinterland thrust systems and activity along the transverse faults. In the study area, the NAT and MBT are characterized by the presence of numerous transverse faults, as mentioned in the text. Further, Kayal (2014) and Kayal et al. (2003) have also indicated presence of the N–S fault, transverse to the MCT (see Fig. S1).

## 5 Discussion

Analysis of present dataset suggests that the Inner Lesser Himalaya and MCT zone accommodate maximum amount of shortening of the India-Eurasia convergence in Uttarakhand Himalaya. The occurrence of maximum seismicity in this part supports our observation. Based on the previous studies a mid-crustal ramp is situated nearly beneath the MCT (see also Molnar 1990; Srivastava and Mitra 1994; Avouac 2003; Yin 2006; Wobus et al. 2006; Caldwell et al. 2013, Negi et al. 2017) in our study region (see Fig. 3b).

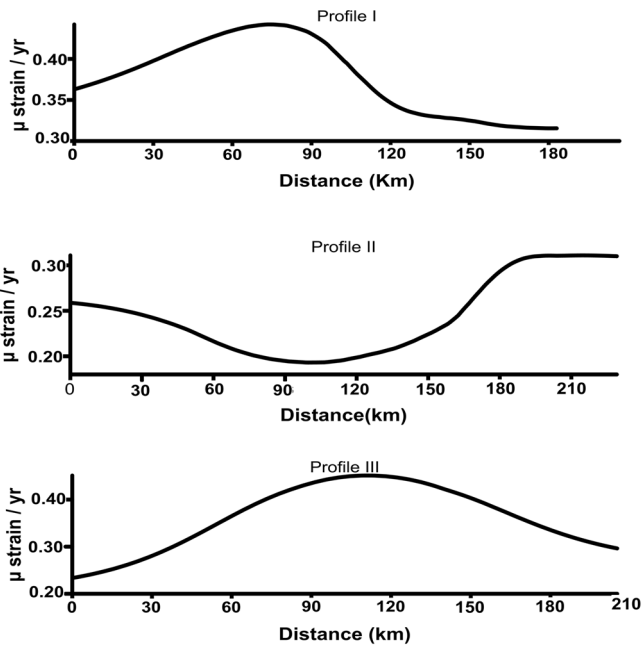
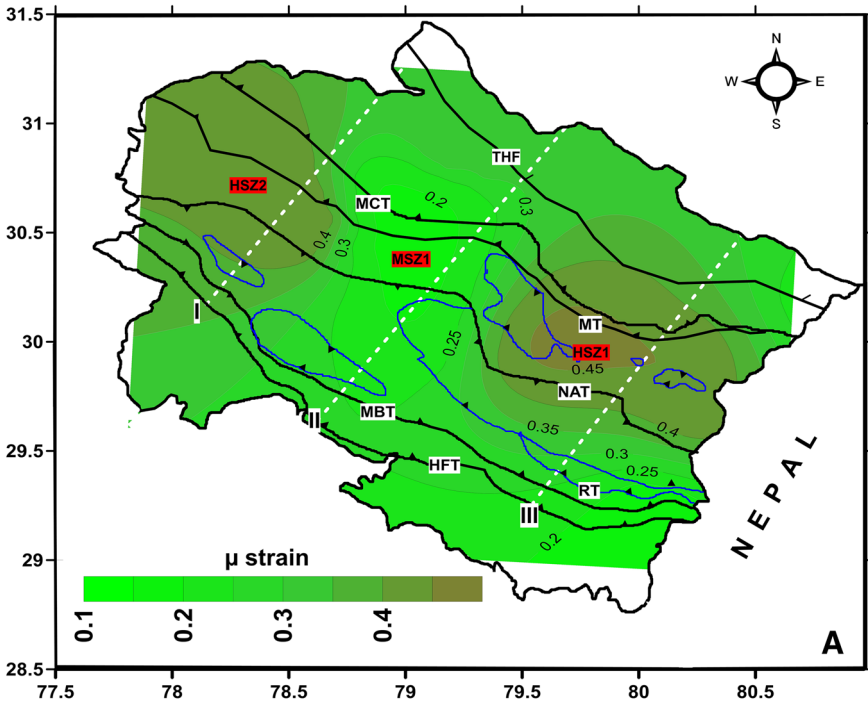
Correlation between the deformation pattern and seismicity indicate a direct relation among them (see Fig. 3b). The arc-perpendicular deformation rate, which is less than 4 mm/year in the Outer Lesser Himalaya reaches up to 12 mm/year in the Inner

**Fig. 4** **a** Calculated strain rate tensor indicating high strain zones (HSZ1 and HSZ2) and moderate strain zones (MSZ1). The zones with strain value  $>0.3$  micro-strain/year are considered as HSZ while  $<0.3$  micro-strain/year are considered as MSZ. The distribution pattern indicates lateral variation in the strain value which is in accordance to the Mahendragar–Dehradun fault based on the gravity analysis (Hetényi et al. 2016). **b** Lateral variation is clearly seen in the 3 profiles starting from the HFT (surface trace of MHT). The profiles I and III point to maximum strain of 0.45 micro-strain/year, at a distance of 80 and 110 km from the HFT. Profile II in the middle of the study area reveals maximum strain of 0.30 micro-strain/year at a distance of 190 km from the HFT

Lesser Himalaya and Higher Himalaya. Therefore, the deformation in this part may be correlated with the ramp structure along the MHT, and suggests that a small part of stress accumulation around the down-dip end is expressed in the form of current seismic activity (Bilham et al. 1998; Banerjee and Bürgmann 2002; Bollinger et al. 2004). The earthquake catalog suggests that Mw 6.3 (Uttarkashi, 1991) and Mw 6.6 (Chamoli, 1999) are the highest magnitude earthquakes in this part during the last three decades. The last great earthquake in this part was probably during the thirteenth century (Rajendran and Rajendran 2011; Rajendran et al. 2015; Jayangondaperumal et al. 2017). In this scenario, the present day deformation rate, if we apply over last 700 year, is sufficient to generate a great earthquake. Based on these circumstances, Nath et al. (2008) have indicated a 10% probability of Mw 8.5 earthquake in the next 50 years in this part of the Himalaya.

The Himalaya, which is considered as a result of compressive tectonics, is mainly believed to sustain the compressional strain. Also, several studies carried out in the different segments of Himalaya support this hypothesis. Based on the strain analysis, our work provides a prominent signal of compressional strain in Uttarakhand Himalaya (Figs. 4, 5). A maximum strain of  $\geq 0.45$  micro-strain/year is observed near the vicinity of the MCT, including parts of the Lesser and Higher Himalaya. The HSZ1 and HSZ2 point to maximum compressional strain of 0.45 micro-strain/year in the study area. An earthquake of M 6.3 in 1991 has already been triggered in the HSZ2. Tectonically, these zones encompass the MCT, MT and NAT. Therefore, we suggest that the seismic activity along these faults systems is related to the maximum strain. Mahesh et al. (2015) correlated seismic activity in this part of Himalaya with the MT and few other transverse faults. The MSZ1 (Fig. 4) that falls in the middle of the study area reveals maximum strain of 0.20 micro-strain/year. The seismic data of this part show occurrences of numerous micro earthquakes (Pathak et al. 2015) and has previously experienced an earthquake of M 6.6 at Chamoli in the year 1999. We believe that the lateral variation in the strain value within the Uttarakhand Himalaya is an indicator of segmented behavior of the Himalayan arc. The seismicity pattern and fault plane solution provide evidence of along-strike variation in the region (Kayal 2001). Along-strike variation in the Moho depth between Garhwal and NW Himalaya has been reported by Caldwell et al. (2013). A gravity-based study (Hetényi et al. 2016) has also identified one such structural segment in the Uttarakhand Himalaya, indicating lateral variation due to inherited structure of the Indian plate.

The seismicity pattern indicates that the earthquakes are more concentrated near the MCT towards the west while, towards the east, these are widely distributed between the THF and MT in the study area. Another important trend is that the earthquakes are closely concentrated in the middle of the study area. We presume that this kind of pattern indicates variation in the locking length of the MHT, and that this is possibly due to the presence of transverse structural features and heterogeneity in the under-thrusting Indian plate (Valdiya 1976; Dasgupta et al. 1987). One such structure is known as



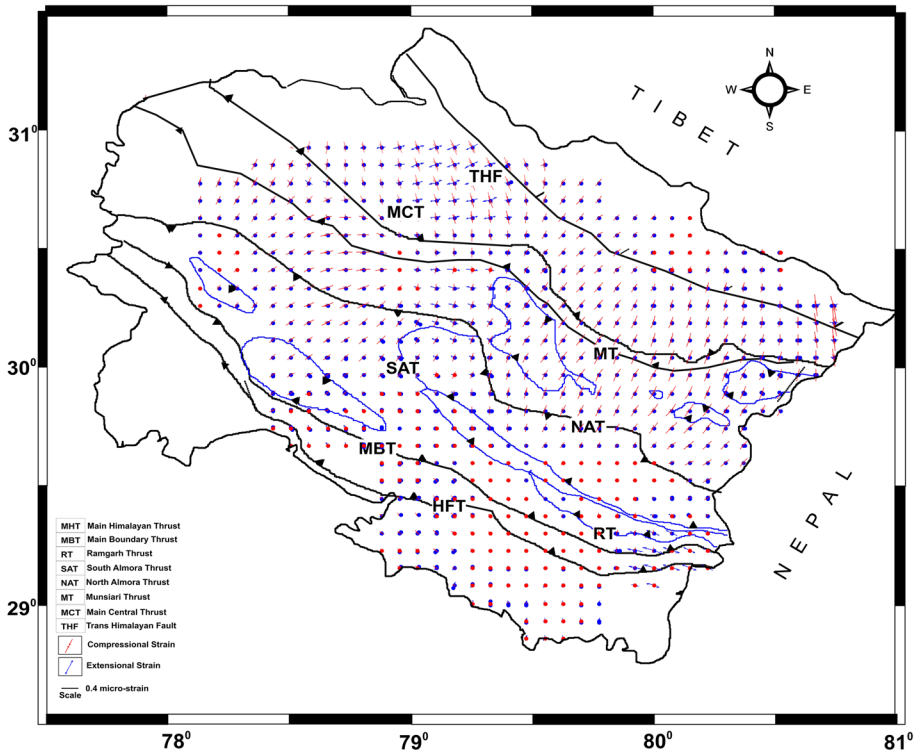


**Fig. 5** Calculated strain rate tensor indicating domination of compressional strain in the area as expected because of the tectonics of the Indian–Eurasia collision. Blue and red tensors represent extension and compression, respectively. (Color figure online)

Delhi–Haridwar ridge based on the seismicity analysis (Arora and Mahashabde 1987; Lyubushin et al. 2010; Roy and Mondal 2012) and Mahendragar–Dehradun Fault based on the gravity analysis (Hetényi et al. 2016) in the Uttarakhand Himalaya.

Although it is a well known fact that earthquakes result from strain buildup of longer time period and GPS results are based on only a few years of data, a comparison between strain accumulation and earthquake distribution suggests a good correlation in the Uttarakhand Himalaya. A number of studies in the different parts of world point out high strain rate in the low earthquake activity areas and vice versa. Analysis of the earthquake dataset (1970–2015) indicates higher concentration in the MSZ1 and lower concentration of earthquakes in the HSZ1 and HSZ2. This clearly infers that some amount of accumulated strain in the MSZ is getting released in form of the earthquakes through the MCT, MT and some local faults. Therefore, based on the comparison between seismicity and strain rate, we can conclude that the seismicity in the HSZ is directly associated with the locked segment of the MHT, whereas part of the seismicity in the MSZ is associated with the motion along the localized faults. In a detailed study of earthquake pattern of Kumaun and Garhwal region, Mahesh et al. (2015) observed a number of localized zones of stress accumulation related to the normal/strike-slip fault motion. The occurrence of a few strike-slip (component of normal/reverse) earthquakes

together with the majority of thrust earthquakes (Stevens and Avouac 2015) indicates activity of the local faults (Figs. S3 and S4).

## 6 Conclusions

On the basis of new GPS data and a compiled dataset, we sum up with the following results on the deformation and strain pattern of Uttarakhand Himalaya.

1. Maximum amount of deformation near the traces of hinterland faults (mainly MCT) suggests excessive accumulation of stress at the down-dip edge of the locked MHT.
2. Most of the Uttarakhand Himalaya encompasses compressional strain and a maximum of 0.45 micro-strain/year is suggested in parts of the Inner Lesser Himalaya and Higher Himalaya.
3. Most crucial finding of the present study is the detection of strain accumulation, and this is categorized into High Strain Zones (HSZ) and Moderate Strain Zones (MSZ1) based on the magnitude of strain.
4. Variation in the strain value suggests along-strike behaviour of the Himalayan arc within Uttarakhand Himalaya and prevailing seismicity and gravity pattern is in agreement with our GPS results.
5. The comparison between seismicity and strain rate suggests that the seismicity in the HSZ is directly associated with the locked segment of the MHT, whereas a part of seismicity in the MSZ is associated with the motion along the localized faults.

**Acknowledgements** The authors are thankful to DG, ISR, Gandhinagar for their encouragement. RKD is grateful to SERB division (DST, New Delhi) for financial support under the fast track scheme (SR/FTP/ES-38/2013). The authors thankfully acknowledge the partial financial assistance from MoES, New Delhi and Science and Technology, Gandhinagar. We thank two anonymous reviewers and Editor György Hetényi for their valuable comments that helped to improve the manuscript.

## References

- Ader T, Avouac JP, Liu-Zeng J, Lyon-Caen H, Bollinger L, Galetzka J, Genrich J, Thomas M, Chanard K, Sapkota S, Rajaure S, Shrestha P, Ding L, Flouzat M (2012) Convergence rate across the Nepal Himalaya and interseismic coupling on the Main Himalayan Thrust: implications. *J Geophys Res* 117:B04403
- Arora BR, Mahashabde MV (1987) A transverse conductive structure in the northwest Himalaya. *Phys Earth Planet Inter* 45:119–127
- Arora BR, Gahalaut VK, Kumar N (2012) Structural control on along-strike variation in the seismicity of the northwest Himalaya. *J Asian Earth Sci* 57:15–24
- Avouac JP (2003) Mountain building erosion and the seismic cycle in the Nepal Himalaya. *Adv Geophys* 46:1–80
- Avouac JP, Tapponier P (1993) Kinematic model of active deformation in Central Asia. *Geophys Res Lett* 20:895–898
- Avouac JP, Lingsen M, Wei S, Wang T, Ampeuro JP (2015) Lower edge of locked Main Himalayan Thrust unzipped by the 2015 Gorkha earthquake. *Nat Geosci* 8:08–711
- Banerjee P, Bürgmann R (2002) Convergence across the northwest Himalaya from GPS measurements. *Geophys Res Lett* 29:30–31. <https://doi.org/10.1029/2002GL015184>

- Banerjee P, Bürgmann R, Nagarajan B, Apel B (2008) Intraplate deformation of the Indian subcontinent. *Geophys Res Lett* 35:L18301
- Bettinelli P, Avouac JP, Flouzat M, Jouanne F, Bollinger L, Willis P, Chitrakar GR (2006) Plate motion of India and interseismic strain in the Nepal Himalayan from GPS and DORIS measurements. *J Geode* 80:567–589
- Bilham R, Larson K, Freymueller J (1997) GPS measurements of present-day convergence across the Nepal Himalaya. *Nature* 386:61–64
- Bilham R, Blume F, Bendick R, Gaur VK (1998) Geodetic constraints on the translation and deformation of India: implications for future great Himalayan earthquakes. *Curr Sci* 74:213–229
- Bilham R, Gaur VK, Molnar P (2001) Himalayan seismic hazard. *Science* 293:1442–1444
- Blewitt G (1989) Carrier phase ambiguity resolution for the global positioning system applied to geodetic baselines up to 2000 km. *J Geophys Res* 94:1187–1203
- Bollinger L, Avouac JP, Cattin R, Pandey MR (2004) Stress buildup in the Himalaya. *J Geophys Res* 109(B11):B11405. <https://doi.org/10.1029/2003JB002911>
- Caldwell WB, Klemperer SL, Lawrence JF, Rai SS, Ashish A (2013) Characterizing the Main Himalayan Thrust in the Garhwal Himalaya India with receiver function CCP stacking. *Earth Plan Sci Lett* 367:15–27
- Cattin R, Avouac JP (2000) Modeling of mountain building and the seismic cycle in the Himalaya of Nepal. *J Geophys Res* 105:13389–13407
- Dasgupta S, Mukhopadhyay M, Nandy DR (1987) Active transverse features in the central portion of the Himalaya. *Tectonophysics* 136:255–264
- Dong DN, Bock Y (1989) GPS network analysis with phase ambiguity resolution applied to crustal deformation studies in California. *J Geophys Res* 94:3949–3966
- Dumka RK (2011) Determination of crustal strain field in Kumaun Himalaya using Global Positioning System (GPS) geodesy. Lambert Academic Publishing, Saarbrücken. ISBN 978-3-8465-0859-6
- Dumka RK, Kotlia BS, Kumar K, Satyal G (2014a) Quantification of crustal strain rate in Kumaun Himalaya (India) using GPS measurements of crustal deformation. *Himal Geol* 35(2):146–155
- Dumka RK, Kotlia BS, Kumar K, Satyal G, Joshi LM (2014b) Crustal deformation revealed by GPS in Kumaun Himalaya India. *J Mount Sci* 11(1):41–50
- Estey LH, Meertens CM (1999) TEQC: the multi-purpose toolkit for GPS/GLONASS data. *GPS Solut* 3:44–49. <https://doi.org/10.1007/PL00012778>
- Gahalaut VK (2008) Major and great earthquakes and seismic gaps in the Himalayan arc. *Mem Geol Soc India* 66:373–393
- Gansser A (1964) *Geology of the Himalaya*. Interscience, New York, pp 1–289
- Godin L (2003) Structural evolution of the Tethyan sedimentary sequence in the Annanpurna area central Nepal Himalaya. *J Asian Earth Sci* 22:307–328
- Hauck ML, Nelson KD, Brown LD, Zhao W, Ross AR (1998) Crustal structure of the Himalayan orogen at 90° east longitude from project INDEPTH deep reflection profiles. *Tectonophysics* 17:481–500
- Heidbach O, Rajabi M, Reiter K, Ziegler M (2016) World stress map 2016. GFZ Data Serv. <https://doi.org/10.5880/WSM.2016.002>
- Herring T, King RW, McClusky SC (2006) GAMIT reference manual GPS analysis at MIT release 103 Department of Earth Atmospheric and Planetary Sciences. Massachusetts Institute of Technology, Cambridge, pp 1–36
- Herring TA, King RW, McClusky SC (2010) Introduction to GAMIT/GLOBK report. Massachusetts Institute of Technology, Cambridge
- Hetényi G, Cattin R, Berthet T, Moigne NL, Chopel J, Lechmann S, Hammer P, Drukpa D, Sapkota SN, Gautier S, Thinley K (2016) Segmentation of the Himalayas as revealed by arc-parallel gravity anomalies. *Sci Rep* 6(33866):1–10. <https://doi.org/10.1038/srep33866>
- ISC, International Seismological Centre (2015) On-line bulletin. International Seismological Centre, Thatcham, United Kingdom, <http://www.isc.ac.uk>. Accessed 7 April 2016
- Jade S (2004) Estimates of plate velocity and crustal deformation in the Indian subcontinent using GPS geodesy. *Curr Sci* 86:1343–1348
- Jade S, Mukul M, Bhattacharyya AK, Vijayan MSM, Saigeetha J, Kumar A, Tiwari RP, Kumar A, Kalita S, Sahu SC, Krishna AP, Gupta SS, Murthy MVRL, Gaur VK (2007) Estimates of inter seismic deformation in Northeast India from GPS measurements. *Earth Planet Sci Lett* 263:221–234
- Jade S, Mukul M, Gaur VK, Kumar K, Shringeshwar TS, Satyal GS, Dumka RK, Jagannathan S, Ananda MB, Kumar PD, Banerjee S (2014) Contemporary deformation in the Kashmir–Himachal Garhwal and Kumaon Himalaya: significant insights from 1995–2008 GPS time series. *J Geod* 88:539–557



- Jade S, Shrungeshwara TS, Kumar K, Choudhury P, Dumka RK, Bhu H (2017) India plate angular velocity and contemporary deformation rates from continuous GPS measurements from 1996 to 2015. *Sci Rep* 7:11439:1–11439:16
- Jayangondaperumal R, Daniels R, Niemi L, Tina M (2017) A paleoseismic age model for large-magnitude earthquakes on fault segments of the Himalayan Frontal Thrust in the Central Seismic Gap of northern India. *Quat Int* 462:130–137. <https://doi.org/10.1016/j.quaint.2017.04.008>
- Jhingran AG, Thakur VC, Tandon SK (1976) Structure and tectonics of the Himalaya (Misc). *Geol Surv India* 41:1–36
- Joshi LM, Kotlia BS (2014) Neotectonically triggered instability around the palaeolake regime in Central Kumaun Himalaya India. *Quat Int* 371:219–231. <https://doi.org/10.1016/j.quaint.2014.10.033>
- Jouanne F, Mugnier JL, Pandey M, Gamond JF, Le Fort P, Serrurier P, Vigny C, Avouac JP (1999) Oblique convergence in Himalaya of western Nepal deduced from preliminary results of GPS measurements. *Geophys Res Lett* 26:1933–1936
- Jouanne F, Mugnier JL, Gamond JP, Le Fort P, Pandey MR, Bollinger L, Flouzat M, Avouac JP (2004) Current shortening across the Himalayas of Nepal. *Geophys J Int* 157:1–14. <https://doi.org/10.1111/j1365-246x.200402180x>
- Kayal JR (2001) Microearthquake activity in some part of the Himalaya and the tectonic model. *Tectonophysics* 339:331–351
- Kayal JR (2014) Seismotectonics of the great and large earthquakes in Himalaya. *Curr Sci* 106:25–28
- Kayal JR, Ram S, Singh OP, Chakraborty PK, Karunakar G (2003) Aftershocks of the March 1999 Chamoli Earthquake and seismotectonic structure of the Garhwal Himalaya. *Bull Seismol Soc Am* 93:109–117
- King RW, Bock Y (1998) Documentation for the GAMIT GPS processing software release 100. Massachusetts Institute of Technology, Cambridge, pp 1–172
- Kotlia BS, Joshi LM (2013) Neotectonic and climatic impressions in the zone of Trans Himadri Fault (THF) Kumaun Tethys Himalaya (India): a case study from palaeolake deposits. *Z Geomorphol* 57(3):289–303. <https://doi.org/10.1127/0372-8854/2013/0057-0101>
- Kotlia BS, Rawat KS (2004) Soft sediment deformation structures in the Garbyang palaeolake: evidence for the past shaking events in the Kumaun Tethys Himalaya. *Curr Sci* 87:377–379
- Kotlia BS, Bhalla MS, Sharma C, Rajagopalan G, Ramesh R, Chauhan MS, Mathur PD, Bhandari S, Chacko ST (1997) Palaeoclimatic conditions in the upper Pleistocene and Holocene Bhimtal-Naukuchial lake basin in southcentral Kumaun North India. *Palaeogeogr Palaeoclimatol Palaeoecol* 130:307–322
- Kotlia BS, Sharma C, Bhalla MS, Rajagopalan G, Subrahmanyam K, Bhattacharyya A, Valdiya KS (2000) Palaeoclimatic conditions in the Late Pleistocene Wadda lake, eastern Kumaun Himalaya (India). *Palaeogeogr Palaeoclimatol Palaeoecol* 162:105–118
- Kotlia BS, Sanwal J, Bhattacharya SK (2008) Climatic record between ca 31 and 22 ka BP in East-Central Uttarakhand Himalaya India. *Himal Geol* 29:25–33
- Kotlia BS, Sanwal J, Phartiyal B, Joshi LM, Trivedi A, Sharma C (2010) Late quaternary climatic changes in the eastern Kumaun Himalaya India as deduced from multi-proxy studies. *Quat Int* 213:44–55
- Kundu B, Yadav R, Bali V, Chodhury S, Gahalaut VK (2014) Oblique convergence and slip partitioning in the NW Himalaya: implications from GPS measurements. *Tectonics* 33:2013–2024. <https://doi.org/10.1002/2014TC003633>
- Larson K, Bürgmann R, Bilham R, Freymueller JT (1999) Kinematics of the India–Eurasia collision zone from GPS measurements. *J Geophys Res* 104:1077–1093. <https://doi.org/10.1029/1998JB900043>
- Lavé J, Avouac JP (2000) Active folding of fluvial terraces across the Siwaliks Hills Himalayas of central Nepal. *J Geophys Res* 105:5735–5770
- Le Fort P (1975) Himalayas: the collided range Present knowledge of the continental arc. *Am J Sci* 275(A):1–44
- Livieratos E (1980) Crustal strains using geodetic methods. *Quaterniones Geodesiae* 3:191–211
- Lyubushin AA, Arora BR, Kumar N (2010) Investigation of seismicity in western Himalaya. *Russ J Geophys Res* 11(1):27–34
- Mahesh P, Catherine JK, Kundu B, Ambikapathy A, Basal A, Premkishor L, Narsaiah M, Ghavri S, Chadha RK, Chodhury P, Singh DK, Kumar S, Nagarajan B, Bhatt BC, Tiwari RP, Kumar A, Bhu A, Kalita S (2012) Rigid Indian plate: constraints from GPS measurements. *Gond Res* 22:1068–1072
- Mahesh P, Gupta S, Saikia U, Rai SS (2015) Seismotectonics and crustal stress field in the Kumaon–Garhwal Himalaya. *Tectonophysics* 655:124–138. <https://doi.org/10.1016/j.tecto.2015.05.016>
- Mao A, Christopher GA, Timothy HD (1999) Noise in GPS coordinate time series. *J Geophys Res* 104:2792–2816
- Mehta JS, Sanwal R (2011) Evidence of active tectonics along oblique transverse normal fault in the Kosi River valley around Betalghat Kumaun Lesser Himalaya India. *Curr Sci* 101:541–543

- Middlemiss CS (1890a) Geological sketch of Nainital with some remarks on natural condition governing the mountain slopes. *Rec Geol Surv India* 21:213–234
- Middlemiss CS (1890b) Physical geology of the sub-Himalaya of Garhwal and Kumaun. *Mem Geol Surv India* 24:159–200
- Molnar P (1990) A review of the seismicity and the rates of the active underthrusting and the deformation of the Himalaya. *J Himal Geol* 1:131–154
- Mugnier JL, Gajurel A, Huyghe P, Jayangondaperumal R, Jouanne F, Upreti B (2013) Structural interpretation of the great earthquakes of the last millennium in the central Himalaya. *Earth Sci Rev* 127:30–47
- Mukul M, Jade S, Bhattacharya AK, Bhusan A (2010) Crustal shortening in convergent orogens: insights from global positioning system (GPS) measurements in northeast India. *J Geol Soc India* 75:302–312
- Nakata T (1982) A photogrammetric study on active faults in the Nepal Himalayas. *J Nepal Geol Soc* 2:67–80
- Nakata T (1989) Active faults of the Himalaya of India and Nepal. *Geol Soc Am (Spec paper)* 232:243–264
- Nath SK, Shukla K, Vyas M (2008) Seismic hazard scenario and attenuation model of the Garhwal Himalaya using near-field synthesis from weak motion seismometry. *J Earth Sys Sci* 117:649–670
- Negi S, Paul P, Cesca B, Kriegerowski M, Mahesh P, Gupta S (2017) Crustal velocity structure and earthquake processes of Garhwal–Kumaun Himalaya: constraints from regional waveform inversion and array beam modeling. *Tectonophysics* 712:45–63
- Nelson K (1996) Partially molten middle crust beneath southern Tibet: synthesis of project INDEPTH results. *Science* 274:1684–1688
- Pandey MR, Tandukar RP, Avouac JP, Lavé J, Massot JP (1995) Evidence for recent interseismic strain accumulation on a mid-crustal ramp in the Central Himalaya of Nepal. *Geophys Res Lett* 22:751–758
- Pandey MR, Tandukar RP, Avouac JP, Vergne J, Héritier Th (1999) Characteristics of seismicity of Nepal and their seismotectonic implications. *J Asian Earth Sci* 17:703–712
- Pathak V, Pant CC, Darmwal G (2015) Geomorphological features of active tectonics and ongoing seismicity of northeastern Kumaun Himalaya, Uttarakhand, India. *J Earth Syst Sci* 124:1143–1157
- Pesci A, Teza G (2007) Strain rate analysis over the central Apennines from GPS velocities: the development of a new free software. *Boll Geod Sci Affini* 56:69–88
- Pesci A, Giordano T, Giuseppe C (2009) Improving strain rate estimation from velocity data of non-permanent GPS stations: the Central Apennine study case (Italy). *GPS Solut* 13:249–261
- Ponraj M, Miura S, Reddy CD, Prajapati SK, Amirtharaj S, Mahajan SH (2010) Estimation of strain distribution using GPS measurements in the Kumaun region of Lesser Himalaya. *J Asian Earth Sci* 39:658–667
- Ponraj M, Miura S, Reddy CD, Amrithraj S, Mahajan SH (2011) Slip distribution beneath the Central and Western Himalaya inferred from GPS measurements. *Geophy J Int* 185:724–736. <https://doi.org/10.1111/j1365-246X201104958x>
- Rajendran K, Rajendran CP (2011) Revisiting the earthquake sources in the Himalaya: perspectives on past seismicity. *Tectonophysics* 504:75–88
- Rajendran CP, John B, Rajendran K (2015) Medieval pulse of great earthquakes in the central Himalaya: viewing past activities on the frontal thrust. *J Geophys Res Solid Earth* 120:1623–1641. <https://doi.org/10.1002/2014JB011015>
- Rana N, Bhattacharya F, Basavaiah N, Pant RK, Juyal N (2013) Soft sediment deformation structures and their implications for late quaternary seismicity on the south tibetan detachment system central Himalaya (Uttarakhand) India. *Tectonophysics* 592:165–174
- Rawat KS, Kotlia BS (2006) Some examples of load and density inversion structures from a part of the Garbyang palaeolake Kumaun Tethys Himalaya. *J Geol Soc India* 71:232–239
- Roy PNS, Mondal SK (2012) Multifractal analysis of earthquakes in Kumaun Himalaya and its surrounding region. *J Earth Syst Sci* 121(4):1033–1047
- Sati SP, Sundriyal YP, Rawat GS (2007) Geomorphic indicators of neotectonic activity around Srinagar (Alaknanda Basin), Uttarakhand. *Curr Sci* 6:824–829
- Satirapod C, Ogaja C, Wang J, Rizos C (2001) An approach to GPS analysis incorporating wavelet decomposition. *Artif Satell* 36(2):27–35
- Seeber L, Armbruster JG (1981) Great detachment earthquakes along the Himalayan arc and long-term forecasting. In: Simpson DE, Richards PG (eds) *Earthquake prediction: an international review*. American Geophysics Union, Washington, pp 215–242
- Shen ZK, Jackson DD (2000) Optimal estimation of geodetic strain rates from GPS data. *EOS Trans AGU* 81(19):S406
- Shen ZK, Jackson DD, Ge BX (1996) Crustal deformation across and beyond the Los Angeles basin from geodetic measurements. *J Geophys Res* 101:27957–27980
- Shrikande M, Rai D, Narayan J, Das J (2006) The March 29 1999 earthquake at Chamoli India. In: 12WCEE2000

- Snay RA, Solar T, Eckl M (2002) Professional surveyor magazine. [www.profsurv.com](http://www.profsurv.com). Accessed 10 March 2018
- Srivastava P, Mitra G (1994) Thrust geometries and deep structure of the outer and lesser Himalaya Kumaon and Garhwal (India) implications for evolution of the Himalayan fold-and-thrust belt. *Tectonophysics* 13:89–109
- Stevens VL, Avouac JP (2015) Interseismic coupling on the main Himalayan thrust. *Geophys Res Lett* 42:5828–5837. <https://doi.org/10.1002/2015GL064845>
- Teza G, Pesci A, Galgaro A (2008) Grid\_strain and grid\_strain3: software packages for strain field computation in 2D and 3D environment. *Comput Geosci* 34:1142–1153
- Thakur VC (1992) *Geology of the western Himalaya*. Pergmon Press, Oxford and New York, pp 1–355
- Thakur VC (2004) Active tectonics of Himalayan frontal thrust and seismic hazard to Ganga Plain. *Curr Sci* 86:1554–1560
- Valdiya KS (1976) Himalayan transverse faults and folds and their parallelism with subsurface structure of north Indian plains. *Tectonophysics* 32:353–386
- Valdiya KS (1979) An outlook of the structural setup of the Kumaun Himalaya. *J Geol Soc India* 20:145–157
- Valdiya KS (1993) Uplift and geomorphic rejuvenation of the Himalaya in the quaternary period. *Curr Sci* 64:873–885
- Valdiya KS (1999) Reactivation of faults and active folds and geomorphic rejuvenation in eastern Kumaun Himalaya: wider implications. *Indian J Geol* 71:53–63
- Valdiya KS (2003) Reactivation of Himalayan frontal fault: implications. *Curr Sci* 85:1031–1040
- Valdiya KS, Kotlia BS (2001) Fluvial geomorphic evidence for late quaternary reactivation of a synclinally folded nappe in Kumaun Lesser Himalaya. *J Geol Soc India* 58(4):303–317
- Wobus CW, Whipple K, Hodges KV (2006) Neotectonics of the central Nepalese Himalaya: constraints from geomorphology detrital  $^{40}\text{Ar}/^{39}\text{Ar}$  thermochronology and thermal modeling. *Tectonophysics* 25(TC401):1–18
- Yin A (2006) Cenozoic tectonic evolution of the Himalayan orogen as constrained by along-strike variation of structural geometry exhumation history and foreland sedimentation. *Earth Sci Rev* 71:1–131
- Zhao W, Nelson KD (1993) Deep seismic reflection evidence for continental underthrusting beneath southern Tibet. *Nature* 366:557–559. <https://doi.org/10.1038/366557a0>